International Research Journal of Engineering and Technology (IRJET) e-ISSN: 2395-0056
Volume: 08 Issue: 08 | Aug 2021 www.irjet.net p-ISSN: 2395-0072

Unbalance Voltage Compensation in an Islanded Microgrid

Neha Narayan Jumde[1], Prof. Praful Tadse[2]

[1]*PG Scholar, Department of Electrical Engineering, Ballarpur Institute of Technology, Ballarpur-Chandrapur, Maharashtra, India*
[2]*Assistant Professor, Department of Electrical Engineering, Ballarpur Institute of Technology, Ballarpur-Chandrapur, Maharashtra, India*

Abstract - *Voltage imbalance, which has negative impacts on electrical equipment, is one of the primary power quality concerns in low-voltage (LV) microgrids. This method uses a unique control strategy to reduce voltage imbalances caused by photovoltaic (PV) and wind turbine systems. The PV system mitigates the voltage imbalance by evaluating its terminal voltage in this study, which eliminates load current sensors. Because of the challenges of load current sensors, this may effectively lower the cost and complexity of the compensation system. A three-phase PV and wind system is the subject of the suggested control technique. The suggested control method calculates compensatory reference currents based on the double synchronous reference frame (DSRF) analysis of the PV and wind system terminal voltage as the inverter detects voltage imbalance at its terminal. As a result, the microgrid receives compensatory currents from the PV-Wind inverter. Simulation studies in the MATLAB 2015 Simulation environment are used to verify the efficiency of the control strategy.*

Key Words: *Voltage control, Voltage Compensation, Islanded Microgrid*

1. INTRODUCTION

One of the primary problems for microgrids is the protection system, which must react to both main grid and microgrid failures. In the first instance, the protection system should cut the microgrid off from the main grid as soon as possible to safeguard the microgrid loads, and in the second situation, the protection system should isolate the smallest section of the microgrid after the fault is cleared [3]. Microsource and load controllers must allow microgrid segmentation, i.e. a design of numerous islands or sub-microgrids. In these circumstances, issues with the protection system's selectivity (false, needless tripping) and sensitivity (undetected defects or delayed tripping) may emerge. The protection of microgrids is primarily concerned with two issues: the first is related to the number of installed DER units in the microgrid, and the second is related to the availability of a sufficient level of short-circuit current in the microgrid's islanded operating mode, as this level may significantly drop after a disconnection from a stiff main grid. The authors of [3] calculated short-circuit currents for radial feeders with DER and discovered that short-circuit currents utilised in over-current (OC) protection relays are dependent on a DER connection point and feed-in power.

Because of these circumstances, the directions and amplitudes of short circuit currents will change. Because of intermittent micro-sources (wind and solar) and periodic load change, the operational conditions of microgrids are always changing. The network topology can also be modified regularly in order to reduce loss or meet other economic or operational goals. In addition, failures in the main grid or inside the microgrid might result in the formation of controlled islands of various sizes and content.

In such cases, relay coordination may be lost, and general OC protection with a single setting group may be insufficient, i.e., selective operation for all potential faults may not be guaranteed. As a result, it's critical to make sure that the settings for OC protection relays account for grid topology as well as variations in location, kind, and quantity of generation.

Otherwise, during an essential situation, an undesired operation or failure may occur. In microgrids dominated by microsources with power electronic interfaces, a new protection philosophy is required to deal with bi-directional power flows and low short-circuit current levels. Setting parameters of relays must be checked/updated on a regular basis to ensure that they are still appropriate..

The MG is separated from the utility grid when in islanded mode. Because the microgrid is not connected to the utility grid, it has no external power source, and the power balance between generation and demand is solely controlled by the microgrid. As a result, maintaining a healthy balance between demand and generation is a difficult endeavour.

Any imbalance between power supply and demand causes voltage and frequency oscillations, which have a significant impact on power system stability when the microgrid is running in islanded mode. Any deviations in the microgrid system might result in system damage, such as severe disruptions and power outages. As a result, ensuring a suitable control strategy in a microgrid system is critical.

Electricity mismatch in MGs with DERs is mostly caused by variations in power generation and variable demands. Because DERs' electricity generation is dependent on environmental circumstances, it might fluctuate over time, causing an imbalance. When power generation exceeds demand, the frequency of the system rises above nominal value; when power generation falls below demand, the frequency of the system falls. These variations in system frequency can result in severe problems with power stability in a microgrid system, as well as incorrect power supply to loads. As a result, suitable control methods must be used in microgrid systems to cope with voltage and frequency variations and maintain the system's dependable and stable functioning.

2. PROPOSED APPROACH AND MODEL

2.1 Proposed Method

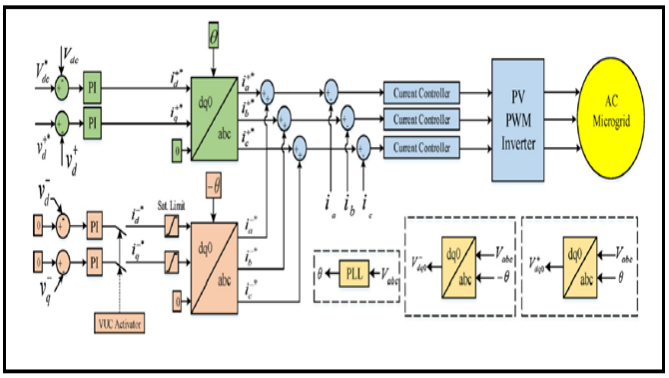

Fig-1: The proposed control system

Fig. 1 The effect of PV involvement in imbalanced current compensation is seen in Figure 5.3. The voltage-controlled voltage sources supply the negative d, q, and zero components of the load current after the unbalanced load is connected to the microgrid.

Negative current components of the unbalanced load create negative voltage components in the PV terminal due to line impedances between these sources and the unbalanced load. Instead of voltage-controlled voltage sources, the PV injects a portion or all of the negative current components to the load terminal once the VUC is activated. As a result, the negative voltages at the load's terminal drop, and the VUF drops as a result.

2.2 MATLAB Simulation Model

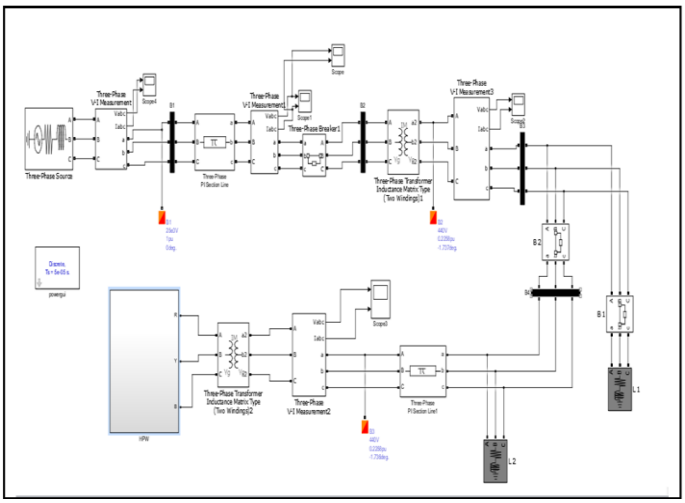

Fig-2: Complete matlab simulation model of proposed system

Table-1: MATLAB Simulation model specification

Sr No	Name of simulation block	Parameter specification
1.	Three phase source	Phase to phase rms voltage = 25 KV, Frequency = 50 Hz, 3 phase short circuit level at base voltage = 100 MVA, Base voltage = 63510.4 V, X/R Ration = 7.
2.	Three phase PI Section Line	Frequency used for RLC line specification = 50 Hz, Positive sequence resistance r1 = 0.01273 Ohm/Km, Zero sequence resistance r0 = 0.3864 Ohm/Km, Positive sequence inductance L1 = 0.9337 mH/Km, Zero sequence inductance L0 = 4.1264 mH/km, Positive sequence capacitance C1 = 12.74 nF/Km, Zero sequence capacitance C2 = 7.751 nF/Km, Line length = 100 Km
3.	Three phase transformer (Distribution Side)	Core type three limb core , Primary winding configuration = Star connected with ground, Secondary winding configuration = Star connected with ground, Nominal power rating = 100 KVA, Nominal supply frequency = 50 Hz, Nominal line to line voltage Primary voltage V1 = 63510.4 V, Secondary Voltage V2 = 254.03 V, Primary winding resistance R1 = 0.01 Per unit, Secondary winding resistance R2 = 0.01 Per Unit, Positive sequence no load loss = 1000 W, Positive sequence short circuit reactance 0.06 pu
4.	Three phase transformer (Renewable energy farm)	Core type three limb core , Primary winding configuration = Star connected with ground, Secondary winding configuration = Star connected with ground, Nominal power rating = 100 KVA, Nominal supply frequency = 50 Hz, Nominal line to line voltage Primary voltage V1 = 254.03 V, Secondary Voltage V2 = 254.03 V, Primary winding resistance R1 = 0.01 Per unit, Secondary winding resistance R2 = 0.01 Per Unit, Positive sequence no load loss = 1000 W, Positive sequence short circuit reactance 0.06 pu

2.3 Solar pv array subsystem model

SUNTECH

Electrical Characteristics

STC	STP285-20/ Wfh	STP280-20/ Wfh	STP275-20/ Wfh
Maximum Power at STC (Pmax)	285 W	280 W	275 W
Optimum Operating Voltage (Vmp)	31.4 V	31.2 V	31.1 V
Optimum Operating Current (Imp)	9.08 A	8.98 A	8.85 A
Open Circuit Voltage (Voc)	38.3 V ±5%	38.1 V ±5%	38.0 V ±5%
Short Circuit Current (Isc)	9.48 A ±5%	9.37 A ±5%	9.24 A ±5%
Module Efficiency	17.2%	16.9%	16.6%
Operating Module Temperature	-40 °C to +85 °C		
Maximum System Voltage	1000 V DC (IEC)		
Maximum Series Fuse Rating	20 A		
Power Tolerance	0/+5 W		

STC: Irradiance 1000 W/m², module temperature 25 °C, AM=1.5;
Best in Class AAA solar simulator (IEC 60904-9) used, power measurement uncertainty is within +/- 3%

Fig-3: Electrical Characteristics of 285 W solar PV module (SUNTECH Manufacturer ratings)

Figure 3 shows the name plate of Suntech solar pv 285 W module specification which utilized for system design. Also figure 4 shows the standard manufacturing PV and VI characteristics for suntech 285 W solar pv module for different solar irradiations. As per name plate specification, solar pv module is design in matlab simulink modeling and analysis of module for different solar irradiation is done. Irradiation is varies from 100 W/m² to 1000 W/m² and PV and VI characteristics observed.

Table-2: Solar pv module specification

Electrical Specification	Values
Module efficiency	14.7%
Power output tolerance	+-3%
Maximum power voltage	35.6 V
Maximum power current	8.02 A
Open circuit voltage Voc	44.7 V
Short circuit current Isc	8.5 A
Peak power Pmax	285 W

Although, there are varies types of solar cell materials, silicon is currently a dominant material utilize in solar cells due to its scalability, momentum and efficiency in light absorption. The fixed PV array has a minimum array size of 5kW. This PV array consists of 4 modules per string connected in series and 4 strings in parallel resulting to 16 modules per array. Each 285W solar panel contains 36 PV cells connected in series as shown in figure 5.2. The parameters of the solar module under study are shown in table 2.

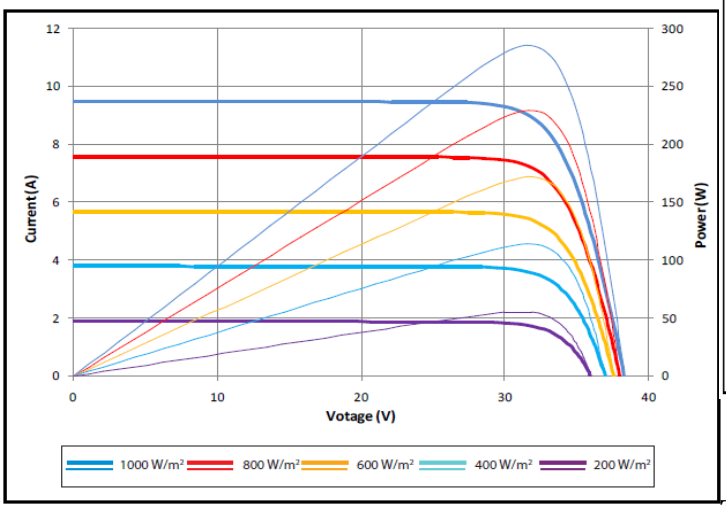

Fig-4: Standard VI and PV characteristics of SUNTECH 285 W solar PV module at different irradiations

Figure 5 shows the name plate of Suntech solar pv 285 W module specification which utilized for system design. Also figure 6 shows the standard manufacturing PV and VI characteristics for suntech 285 W solar pv module for different solar irradiations. As per name plate specification, solar pv module is design in matlab simulink modeling and analysis of module for different solar irradiation is done.

Irradiation is varies from 100 W/m² to 1000 W/m² and PV and VI characteristics observed.

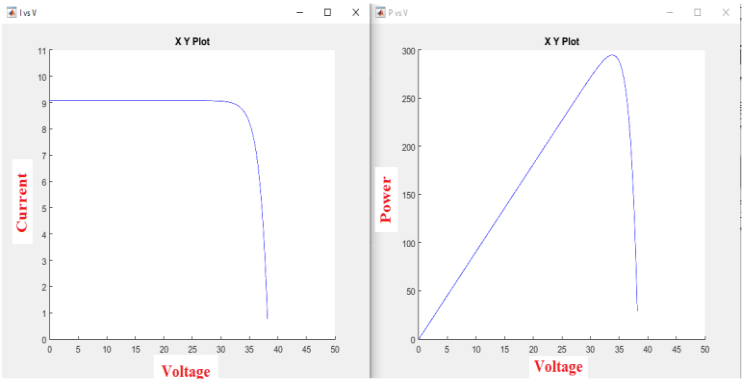

Fig-5: VI and PV characteristics of SUNTECH 285 W solar PV module at 1000 W/m² irradiation using MATLAB simulink modeling

2.4 Wind turbine subsystem model

Figure 6 shows the MATLAB simulink model of wind turbine system with AC generator coupled with wind turbine system model. Wind turbine is provide the mechanical torque Tm as mechanical output and corresponding inputs are Generator speed in pu, Pitch angle in delta and wind speed in m/s.

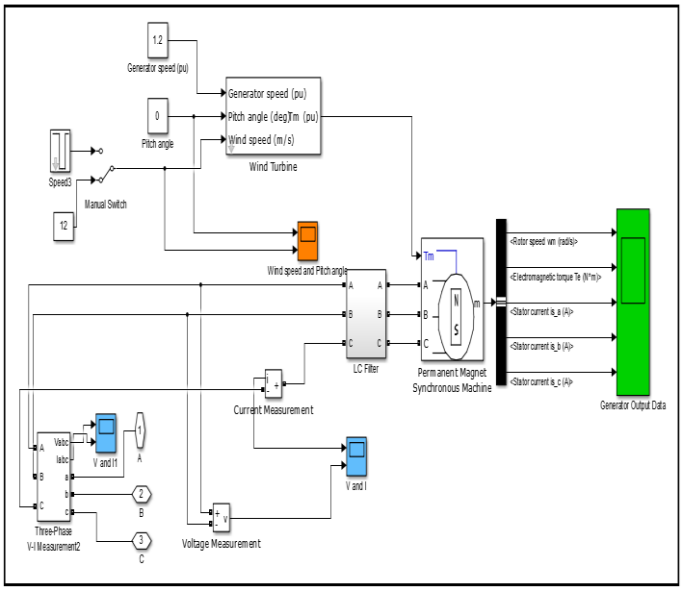

Fig-6: MATLAB Simulink subsystem for wind turbine system

The generated AC three phase supply is not perfect ac supply because of harmonics content present in supply. That output supply is then fed to the LC filter so that harmonics content is minimize and supply then fed to the coupling transformer of transmission line.

Table-3: Parameter specification of wind turbine subsystem model

Sr No	Name of simulink block	Parameters
1	Wind turbine	Nominal mechanical output power =

		200W; Base power of the electrical generator = 222 VA; Base wind speed = 12 m/s; Maximum power at base wind speed = 0.73 pu; Base rotational speed = 1.2 pu;
2	Permanent magnet synchronous machine	Number of phases = 3; Rotor type = Round; Mechanical input = Torque; Present model: 0.8 Nm, 300 V DC, 3000 RPM
3	LC Filter	Inductance L = 20 mH; Capacitive load C: Nominal Phase to phase voltage Vn = 380V; Nominal frequency fn = 50Hz; Capacitive reactive power Qc = 3 KVAr

2.5 Inverter controller subsystem

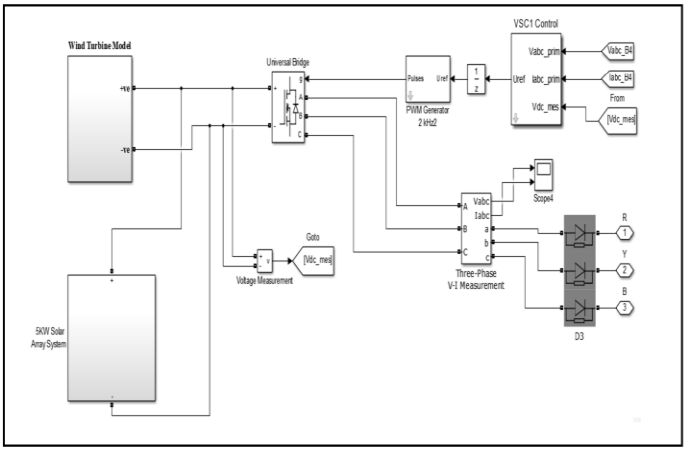

Fig-7: Simulation model with inverter subsystem and controller

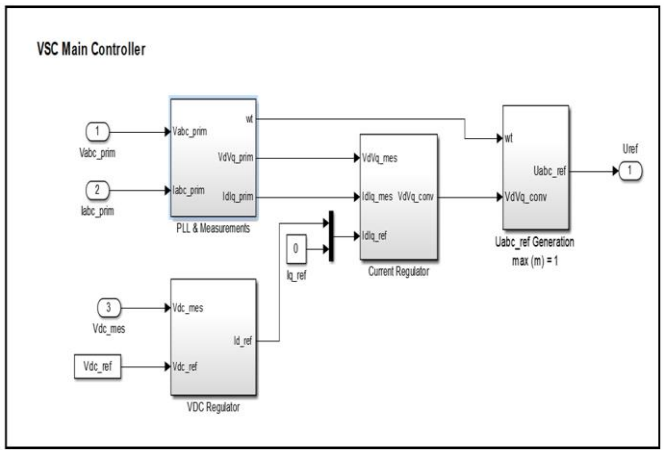

Fig-8: MATLAB simulation model of controller

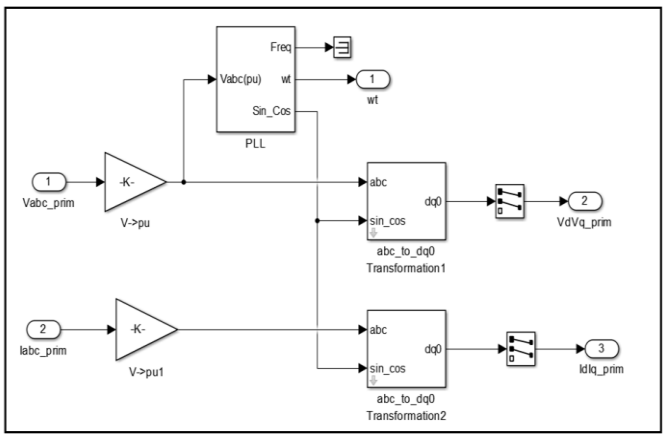

Fig-9: Direct axis and Quaderaure axis component calibration subsystem for controller

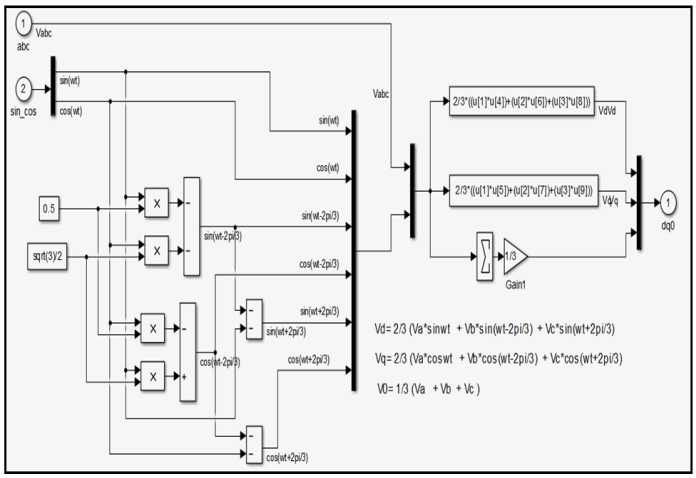

Fig-10: Three phase voltage to direct axis and quaderature axis conversion subsystem

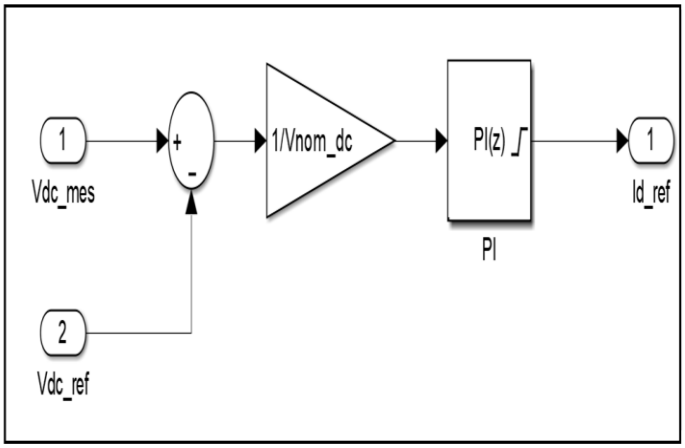

Fig-11: Vdc to Direct axis component calibration

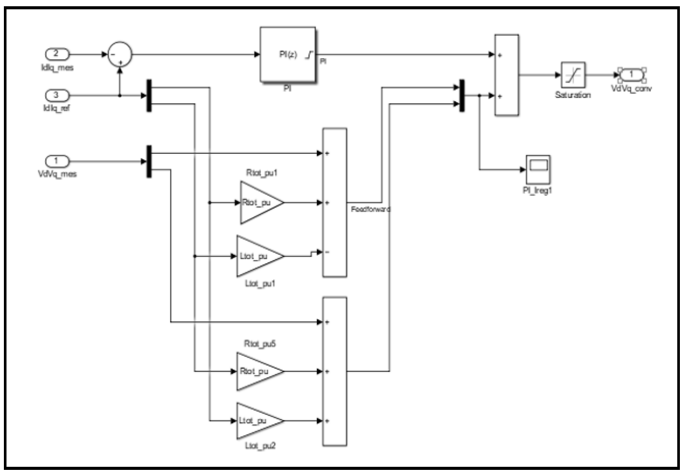

Fig-12: Current controller subsystem matlab simulation model

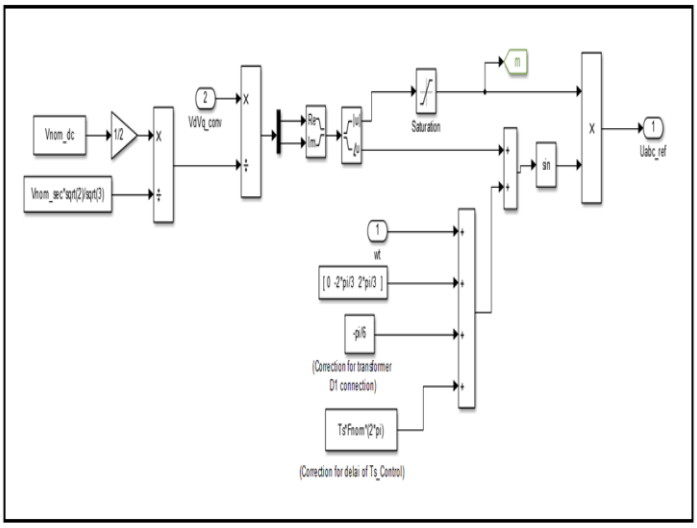

Fig-13: Simulation model for reference voltage generation in controller subsystem

3. SIMULATION RESULTS

3.1 Case-1: Islanding occurs at 0.5 second

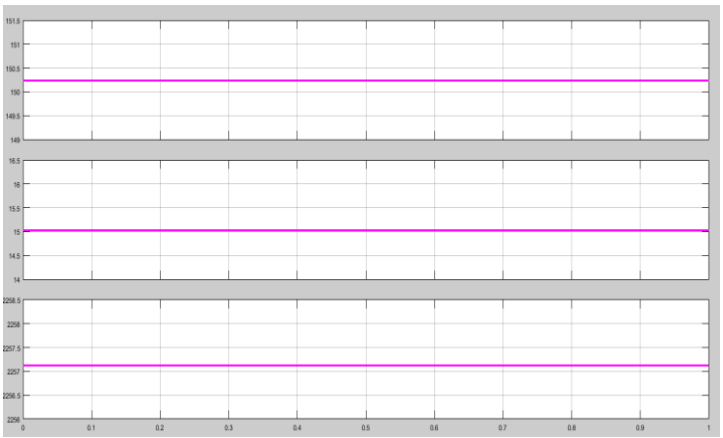

Fig-14: Solar pv system output voltage, output current and output power during case-1

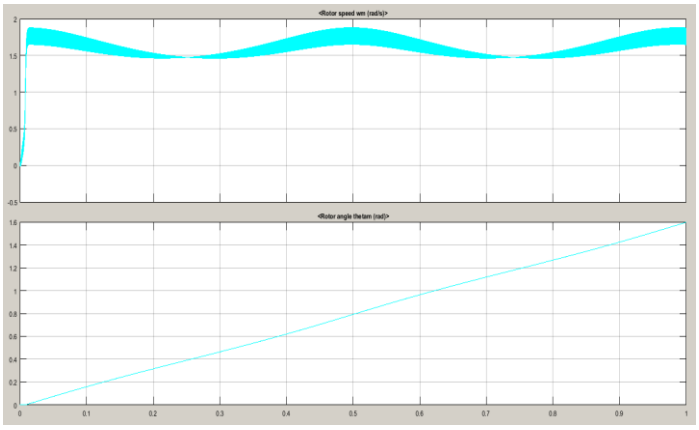

Fig-15: Wind turbine system rotor speed in rad/sec and rotor angle in Rad during case-1

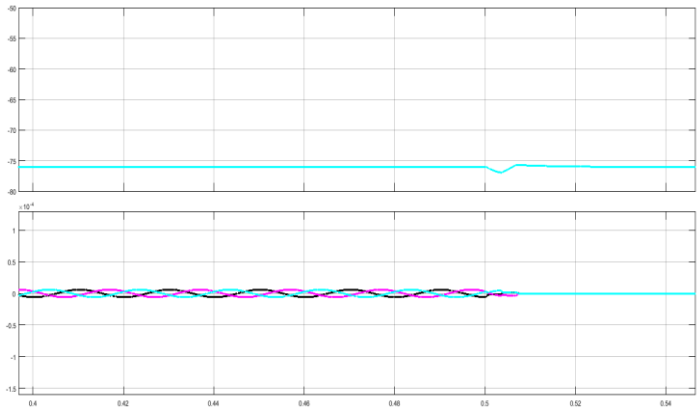

Fig-16: Three phase RMS voltage and current generated by solar pv system and wind turbine system during case-1

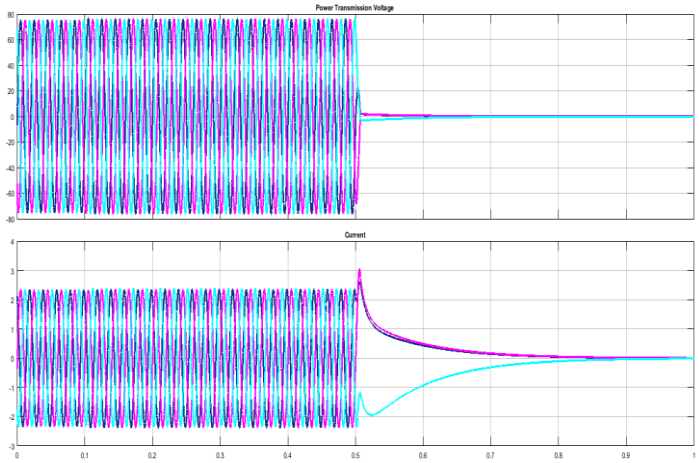

Fig-17: Three phase voltage and current of system during case-1

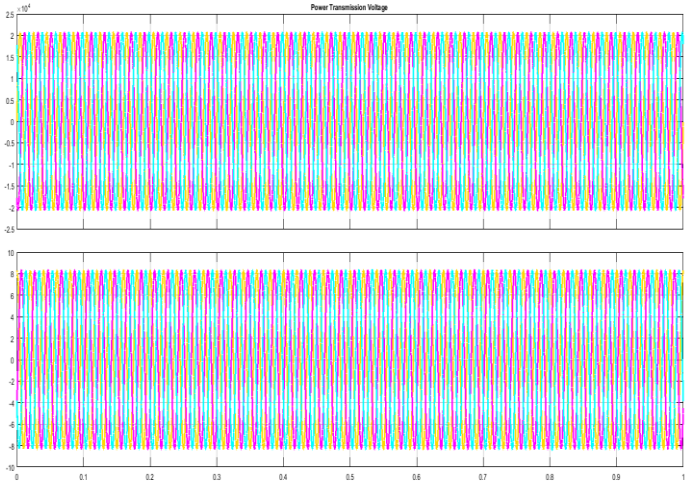

Fig-18: Three phase rms voltage and current of power system at bus bar 1 during case-1

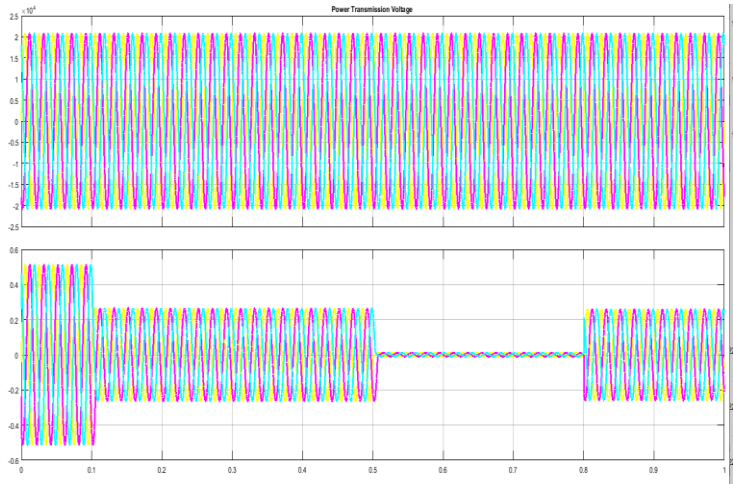

Fig-19: Three phase rms voltage and current of power system at bus bar 2 during case-2 during case-1

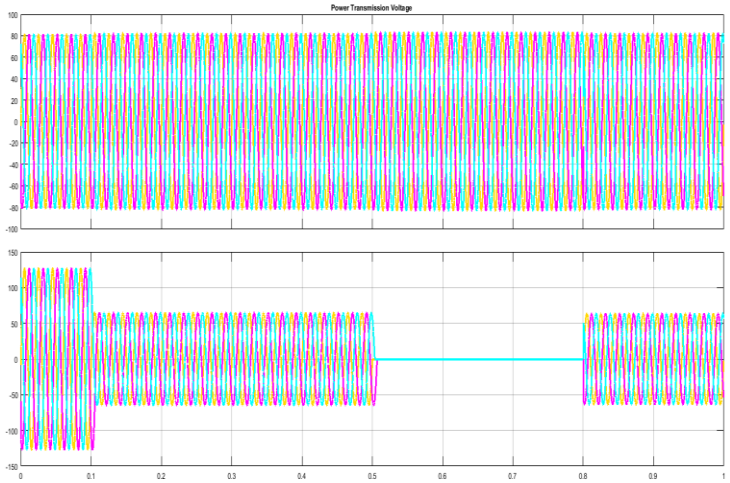

Fig-20: Three phase rms voltage and current of power system at bus bar 3 during case-1

3.2 Case-2: Normal condition without islanding

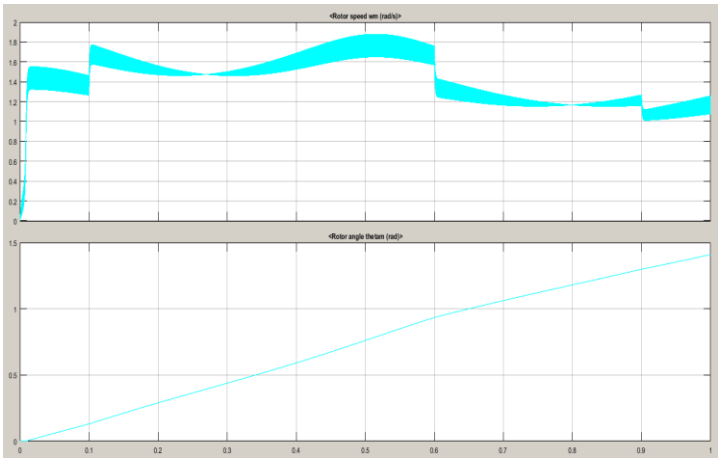

Fig-21: Wind turbine system rotor speed in rad/sec and rotor angle in Radian during case-2

Fig-22: Solar pv system output voltage, output current and output power during case-2

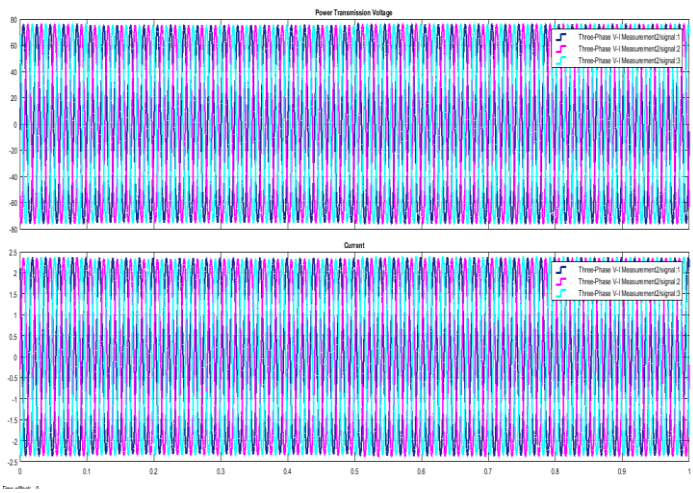

Fig-23: Three phase voltage and current of system generated by wind and solar pv system during case-2

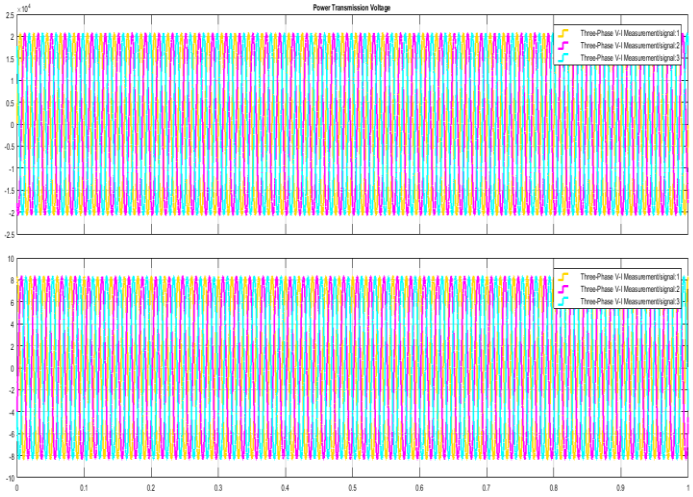

Fig-24: Three phase rms voltage and current of power system at bus bar 1 during case-2

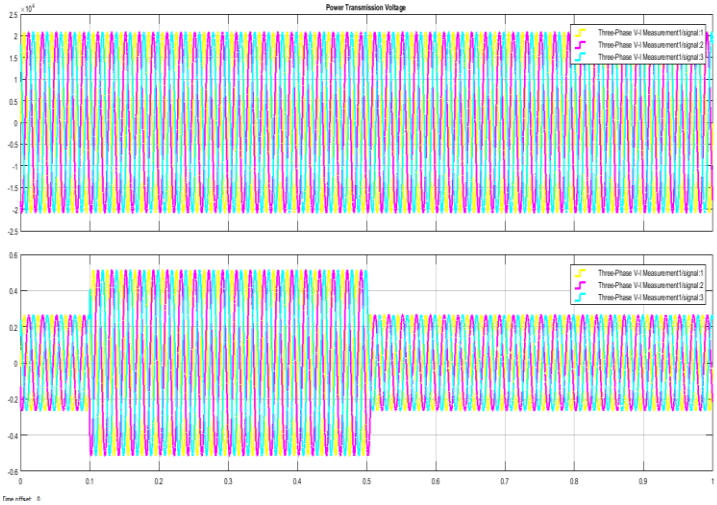

Fig-25: Three phase rms voltage and current of power system at bus bar 2 during case-2

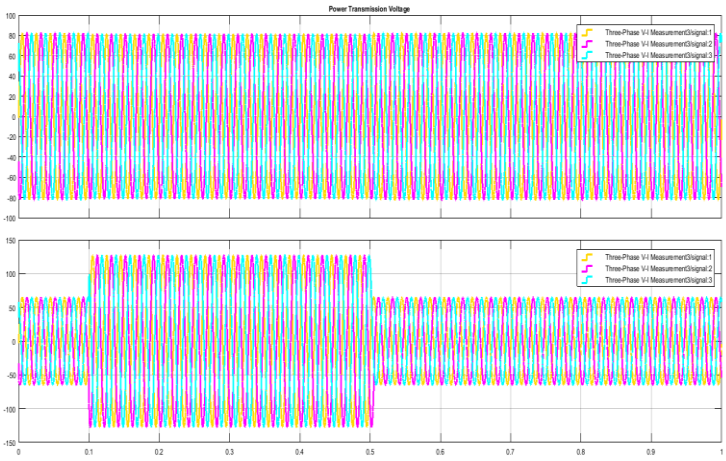

Fig-26: Three phase rms voltage and current of power system at bus bar 3 during case-2

4. CONCLUSIONS

To reduce voltage imbalance, a new control method for a three-phase four-wire PV and wind inverter was proposed in this study. In contrast to APFs, the load current sensor was removed, and the compensation method computed the reference currents by evaluating the PV terminal voltage, lowering the cost and complexity. The double synchronous reference frame (DSRF), which detects the positive and negative sequence of the PV terminal voltages, aided the suggested control method. When an unbalanced load connects to the network, the control system detects negative sequence voltages, which indicates a voltage imbalance.

The control system calculates the needed negative sequence compensating current based on these voltages in order to decrease the voltage imbalance at the PV terminal. Because this control approach does not need the measurement of imbalanced load current, the compensation system might be used without the use of local load current sensors. Although employing the PV inverter as an active power filter might lower the cost of the compensating system, the suggested control method could cut the compensation cost even further. The control scheme's efficacy was tested in the MATLAB 2015 environment.

The simulated scenarios confirmed that the PV system could reduce voltage imbalances while unbalanced loads join to or detach from the LV microgrid. While the suggested control approach was designed for islanded microgrids, it may be used to any distribution network experiencing voltage imbalance.

We must create a solar pv system simulation model in Matlab. The results of a solar pv system, such as VI, PV characteristics, and solar system parameters, were also examined. We must create a wind turbine system. The wind turbine system characteristics, as well as the output voltage and current analysis, were also evaluated. The findings of the wind turbine were evaluated for both constant and variable wind speeds. The inverter subsystem with controller is intended to enhance voltage profile.

REFERENCES

[1] Savaghebi, M., Jalilian, A., Vasquez, J. C., & Guerrero, J. M. (2012). Autonomous voltage unbalance compensation in an islanded droop-controlled microgrid. IEEE Transactions on Industrial Electronics, 60(4), 1390-1402.

[2] Savaghebi, Mehdi, et al. "Secondary control scheme for voltage unbalance compensation in an islanded droop-controlled microgrid." IEEE Transactions on Smart Grid 3.2 (2012): 797-807.

[3] Meng, Lexuan, et al. "Tertiary control of voltage unbalance compensation for optimal power quality in islanded microgrids." IEEE Transactions on Energy Conversion 29.4 (2014): 802-815.

[4] Lu, J., Nejabatkhah, F., Li, Y., & Wu, B. (2014, September). DG control strategies for grid voltage unbalance compensation. In 2014 IEEE Energy Conversion Congress and Exposition (ECCE) (pp. 2932-2939). IEEE.

[5] Tang, F., Zhou, X., Meng, L., Guerrero, J. M., & Vasquez, J. C. (2014, February). Secondary voltage unbalance compensation for three-phase four-wire islanded microgrids. In 2014 IEEE 11th International Multi-Conference on Systems, Signals & Devices (SSD14) (pp. 1-5). IEEE.
[6] Zhao, X., Wu, X., Meng, L., Guerrero, J. M., & Vasquez, J. C. (2015, March). A direct voltage unbalance compensation strategy for islanded microgrids. In 2015 IEEE Applied Power Electronics Conference and Exposition (APEC) (pp. 3252-3259). IEEE.
[7] Meng, L., Zhao, X., Tang, F., Savaghebi, M., Dragicevic, T., Vasquez, J. C., & Guerrero, J. M. (2015). Distributed voltage unbalance compensation in islanded microgrids by using a dynamic consensus algorithm. IEEE Transactions on Power Electronics, 31(1), 827-838.
[8] Savaghebi, M., Shafiee, Q., Vasquez, J. C., & Guerrero, J. M. (2015, July). Adaptive virtual impedance scheme for selective compensation of voltage unbalance and harmonics in microgrids. In 2015 IEEE Power & Energy Society General Meeting (pp. 1-5). IEEE.
[9] Han, Y., Shen, P., Zhao, X., & Guerrero, J. M. (2016). An enhanced power sharing scheme for voltage unbalance and harmonics compensation in an islanded AC microgrid. IEEE Transactions on Energy Conversion, 31(3), 1037-1050.
[10] Ranjbaran, A., and M. Ebadian. "A power sharing scheme for voltage unbalance and harmonics compensation in an islanded microgrid." Electric Power Systems Research 155 (2018): 153-163.
[11] I. Şerban and C. Marinescu, "Frequency control issues in microgrids with renewable energy sources," 2011 7TH INTERNATIONAL SYMPOSIUM ON ADVANCED TOPICS IN ELECTRICAL ENGINEERING (ATEE), Bucharest, 2011, pp. 1-6
[12] L. Kafle, Zhen Ni, R. Tonkoski and QiquanQiao, "Frequency control of isolated microgrid using a droop control approach," 2016 IEEE International Conference on Electro Information Technology (EIT), Grand Forks, ND, 2016, pp. 0771-0775.
[13] A. Klem, M. H. Nehrir and K. Dehghanpour, "Frequency stabilization of an islanded microgrid using droop control and demand response," 2016 North American Power Symposium (NAPS), Denver, CO, 2016, pp. 1-6.
[14] M. Rahmani and M. Goodarzi, "A new controller for frequency protection of an islanded microgrid," 2015 30th International Power System Conference (PSC), Tehran, 2015, pp. 118- 122.
[15] T. Ota, K. Mizuno, K. Yukita, H. Nakano, Y. Goto and K. Ichiyanagi, "Study of load frequency control for a microgrid," 2007 Australasian Universities Power Engineering Conference, Perth, WA, 2007, pp. 1-6.
[16] B. S. Kumar, S. Mishra, C. N. Bhende and M. S. Chauhan, "PI controller based frequency regulator for distributed generation," TENCON 2008 - 2008 IEEE Region 10 Conference, Hyderabad, 2008, pp. 1-6.
[17] G. Mallesham, S. Mishra and A. N. Jha, "Ziegler-Nichols based controller parameters tuning for load frequency control in a microgrid," 2011 International Conference on Energy, Automation and Signal, Bhubaneswar, Odisha, 2011, pp. 1-8.
[18] R. H. Kumar and S. Ushakumari, "Biogeography based tuning of PID controllers for Load Frequency Control in microgrid," 2014 International Conference on Circuits, Power and Computing Technologies [ICCPCT-2014], Nagercoil, 2014, pp. 797-802.
[19] Y. Ma, P. Yang, Y. Wang, S. Zhou and P. He, "Frequency control of islanded microgrid based on wind-PV-diesel-battery hybrid energy sources," 2014 17th International Conference on Electrical Machines and Systems (ICEMS), Hangzhou, 2014, pp. 290-294.
[20] S. Janani and C. Muniraj, "Fuzzy control strategy for microgrids islanded and grid connected operation," 2014 International Conference on Green Computing Communication and Electrical Engineering (ICGCCEE), Coimbatore, 2014, pp. 1-6.
[21] M. Marzband, A. Sumper, O. Gomis-Bellmunt, P. Pezzini and M. Chindris, "Frequency control of isolated wind and diesel hybrid MicroGrid power system by using fuzzy logic controllers and PID controllers," 11th International Conference on Electrical Power Quality and Utilisation, Lisbon, 2011, pp. 1-6.
[22] M. S. Bisht and Sathans, "Fuzzy based intelligent frequency control strategy in standalone hybrid AC microgrid," 2014 IEEE Conference on Control Applications (CCA), Juan Les Antibes, 2014, pp. 873-878.
[23] M. Marzband, A. Sumper, O. Gomis-Bellmunt, P. Pezzini and M. Chindris, "Frequency control of isolated wind and diesel hybrid MicroGrid power system by using fuzzy logic controllers and PID controllers," 11th International Conference on Electrical Power Quality and Utilisation, Lisbon, 2011, pp. 1-6.